



A Filtering Coaxial Probe for Passive Intermodulation Characterization

BAI Yongjiang¹, YANG Jiye¹, ZHU Shaohao²,
YANG Ye², YE Ming¹

(1. Xi'an University of Architecture and Technology, Xi'an 710055, China;
2. ZTE Corporation, Shenzhen 518057, China)

DOI: 10.12142/ZTECOM.202404009

<https://kns.cnki.net/kcms/detail/34.1294.TN.20241029.1436.002.html>,
published online October 29, 2024

Manuscript received: 2024-06-05

Abstract: Passive intermodulation (PIM) in communication systems is an unwanted interference caused by weak nonlinear current-voltage characteristics of radio frequency (RF) passive components. Characterization of PIM is important for both the study of PIM mechanisms and the location/suppression of PIM sources. PIM probes, made of open-ended coaxial transmission lines, have almost the same coupling strength to carriers and PIM products, and are usually used for near-field PIM characterization. Namely, it doesn't have any filtering capability. Therefore, it cannot stop the carrier power from entering into PIM tester's receiver, which may trigger active intermodulation of the receiver and degrade the PIM tester's performance. To overcome this drawback, a passive filtering coaxial probe is proposed here. Compared with existing passive coaxial PIM probes, it has stronger coupling strength for PIM products than for carriers. Thus, the probe itself can block part of the carrier power entering into the PIM tester's receiver. This advantage helps improve PIM tester's overall performance. Both theoretical analysis and experiments are conducted for demonstration. The proposed probe brings more possibility to PIM characterization.

Keywords: coupling gap; passive intermodulation; filtering coaxial probe

Citation (Format 1): BAI Y J, YANG J Y, ZHU S H, et al. A filtering coaxial probe for passive intermodulation characterization [J]. *ZTE Communications*, 2024, 22(4): 59 – 66. DOI: 10.12142/ZTECOM.202404009

Citation (Format 2): Y. J. Bai, J. Y. Yang, S. H. Zhu, et al., "A filtering coaxial probe for passive intermodulation characterization," *ZTE Communications*, vol. 22, no. 4, pp. 59 – 66, Dec. 2024. doi: 10.12142/ZTECOM.202404009.

1 Introduction

Passive intermodulation (PIM) refers to the new output signals generated when two or more high-power carrier signals pass through radio frequency (RF) passive components with weak nonlinear current-voltage characteristics. When PIM products fall into the frequency band of a receiver, the sensitivity of communication systems may be reduced^[1]. In recent years, due to its negative effect on mobile communications^[2], aerospace^[3], military and other fields^[4], research on PIM has attracted much attention from both industry and academia.

At present, the research on PIM mainly focuses on the physical mechanisms^[5], detection^[6–8], suppression^[9] and modeling^[10]. The physical mechanisms of PIM include material nonlinearity and contact nonlinearity. Due to its complexity, the physics behind PIM behavior of RF components/systems is not yet well understood, and thus, it is not easy to model PIM quantitatively. So, the PIM tester is an indispensable diagnostic tool for PIM researchers/engineers.

Regarding PIM measurement, PIM includes conducted PIM (e.g., RF connectors and cables) and radiated PIM (e.g., antennas). With the development of RF systems, some non-

conventional test methods of PIM have been proposed, such as the near-field detection method^[11], the RF cancellation method^[12] and the acoustic vibration method^[13]. Suppression of PIM is the ultimate goal of PIM research and characterization.

Near-field detection of PIM, the purpose of this work, has the potential to find out locations/sources of PIM in a real RF system which is beneficial for suppression of PIM by either hardware-based or software-based methods. For example, there may be multiple PIM sources in a complicated RF system, like a rusted/loose RF connector, or a cracked microstrip line. If one can locate the PIM source, efforts can be made to suppress it/them. To develop such a tool, many kinds of PIM probes for near-field PIM detection have been studied, including the electromagnetic probe^[11], the antenna probe^[14], the print circuit board (PCB) probe^[15], the waveguide probe^[16], etc. Each kind of PIM probes has its own pros and cons. For example, the electromagnetic probe usually has a higher spatial resolution. The antenna probe usually has relatively larger detection distance. Here, the detection distance refers to the distance between the PIM probe and the device under test (DUT). The waveguide probe in

Ref. [16] is efficient for the measurement duration since it only needs two one-dimensional scans for a two-dimensional PIM mapping result.

All of the passive and active probes mentioned above have no filtering capability. In other words, to some degree, they are wideband probes. When these probes are used for PIM location, they couple both high-level carriers and low-level PIM products. Thus, to avoid exciting the nonlinearity of PIM testers' receivers, a high-performance duplexer with stringent specifications on both the PIM level and frequency selectivity is required. For example, the out-of-band rejection of the duplexer used in a PIM test system is usually at least 100 dB.

In this paper, a passive filtering PIM probe based on a half-wavelength coaxial transmission line resonator is proposed. Theoretical analysis, electromagnetic simulation and experimental measurement are conducted to demonstrate the probes' working principle and its potential advantages over conventional passive non-filtering PIM probes. The most important difference of the proposed probe is that its coupling strength of PIM products can be higher than that of carriers. As described below, this unique characteristic is expected to be beneficial for improving PIM testers' performances such as larger dynamic range, lower requirement on components, more flexibility, and lower cost.

2 Principle and Theory

2.1 Principle of the Proposed Probe

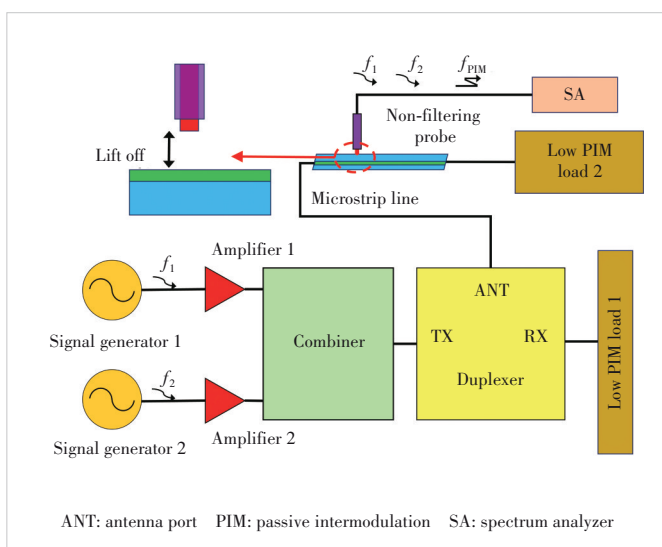
In a typical near-field PIM test system, two signal generators output two sinusoidal signals (denoted as carriers in a PIM community) with the same power but different frequencies, as shown in Fig. 1. After being amplified by power am-

plifiers (PA), the two carriers are combined to form a dual-tone and high-power excitation signal finally input into the transmit port of a low-PIM duplexer with high-performance. Then, high-power carriers output from the antenna port of the duplexer and enter into the DUT (here, a microstrip line is used for demonstration). Both the high-power carriers and the generated forward PIM of the DUT will be absorbed by the low PIM load connected with the DUT. The generated reverse PIM goes back to the antenna port of the duplexer and it can be detected at the receive port of the duplexer.

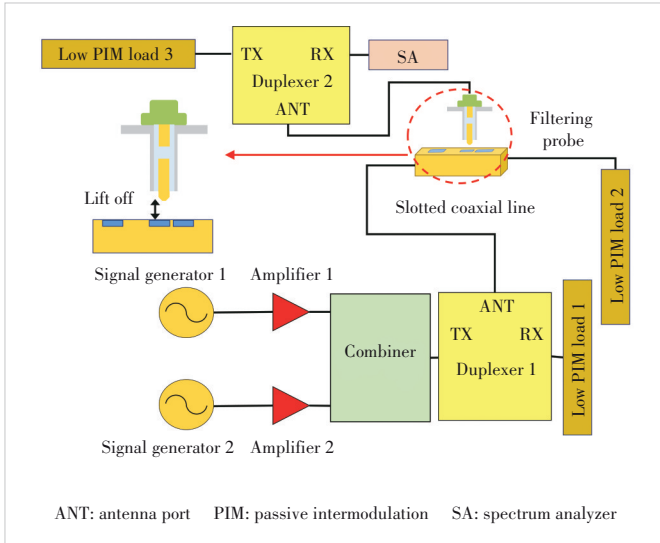
At the same time, both the carriers and the PIM products enter into the near-field PIM probe after experiencing a specific but almost the same attenuation (equal to the insertion loss between the input port of DUT and the output port of the PIM probe), which is quantitatively specified by coupling strength. Usually, coupling strength is mainly determined by the lift-off distance L_l of the PIM probe as shown in Fig. 1. Finally, all of these signals go into the receiver, represented by a spectrum analyzer (SA) here. In this conventional PIM test system, it is obvious that stronger coupling strength means lower insertion loss for both the carriers and PIM products. On one side, the former suggests lower minimum detectable PIM level; on the other side, the latter indicates higher carrier power entering into SA, which may ignite SA's nonlinearity and thus degrade the system's noise floor, increasing the minimum detectable PIM level. This trade-off limits the performance or design flexibility of the conventional PIM test system.

To overcome this trade-off, a low PIM filter/duplexer is usually added between the PIM probe and the SA to filter out the carriers. Since the carriers entering into the probe are attenuated by the added filter/duplexer, it is less likely to excite an observable intermodulation of the SA. However, due to the strong nonlinearity of SA, requirements on the filter/duplexer may be stringent. Thus, when designing a PIM tester with a conventional PIM probe, one may need to pay much attention to the specifications of the filter/duplexer as well as SA.

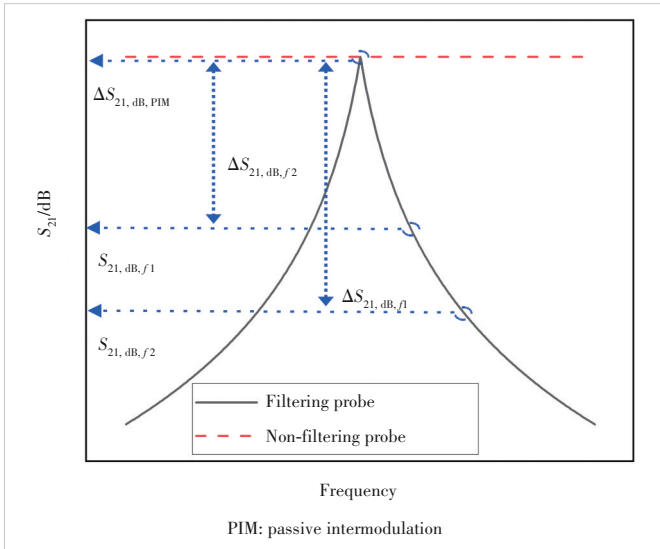
To lighten the burden of the filter/duplexer/SA in a PIM tester, a half wavelength coaxial transmission line-based PIM probe is introduced due to its filtering capability, as shown in Fig. 2. Compared with the conventional PIM probe in Fig. 1, which is made of coaxial transmission line without any frequency selectivity, the proposed probe is essentially a resonator and thus it has frequency selectivity. In detail, with proper design parameters, the proposed filtering PIM probe has a resonant peak close to the frequency of the desired PIM, as shown in Fig. 3. It should be noted that the y-axis in Fig. 3, S_{21} , represents transmission S-parameters between the input port of DUT and the port of PIM probes. The filtering PIM probe has a stronger coupling strength of PIM than that of carriers. In other words, the filtering PIM probe can block the carriers, avoiding/suppressing the excitation



▲ Figure 1. Schematic diagram of near-field PIM test systems based on a non-filtering PIM probe (usually, there is a duplexer between the probe and SA)



▲ Figure 2. Schematic diagram of the near-field PIM test system based on a filtering PIM probe



▲ Figure 3. Schematic diagram of transmission S -parameters between the input port of the device under test (DUT) and the output port of the PIM probe

of active nonlinearity of SA.

Compared with conventional probes, the advantage of the filtering PIM probe may bring the following improvements. First, carriers with higher power can be used because this increase in carrier power will be attenuated by the filtering probe. For example, suppose the acceptable output carrier power at the probe's port (this specification ensures avoiding nonlinearity of SA) is 0 dBm and the filtering probe has 10 dB larger attenuation to carriers than non-filtering probes. Then, if the PIM test system works well for non-filtering probes when carriers' power at the input port of DUT is 43 dBm, the system is expected to work well too for filtering probes when input carrier power to DUT is 53 dBm.

Second, the PIM test system equipped with filtering probes has a higher sensitivity than its non-filtering counterpart. Here, sensitivity means the measurable lowest PIM level. Suppose the noise floor of SA is -125 dBm. To ensure the stability of measurement results, the measurable lowest power of the SA is set to -115 dBm (10 dB higher than the noise floor, known as the 10 dB rule). We suppose the acceptable coupling strength of the non-filtering probe is 30 dB (stronger coupling will excite nonlinearity of SA), which indicates the sensitivity is -85 dBm. For filtering probes, as mentioned above, assuming that the filtering probe has a 10 dB larger attenuation to carriers than non-filtering probes (their attenuation at the PIM frequency is the same), the acceptable coupling strength of the filtering probe is 20 dB which indicates the sensitivity is -95 dBm, 10 dB higher than its non-filtering counterpart.

A similar analysis also shows that the PIM test system using filtering probes has lower requirements on out-of-band rejection specification of filter/duplexer and on intermodulation specifications of SA. Even more, if the filtering probe has enough frequency selectivity, it may be possible to block the carriers going into the SA absolutely and thus one can remove the filter/duplexer, which will be helpful for system integration. A thorough analysis will be detailed in the subsequent subsection.

2.2 Theoretical Analysis

Assuming that the transmission S -parameter S_{21} from the input port of DUT to the output port of PIM probes for carrier 1, carrier 2 and PIM is $S_{21,\text{dB},f1}$, $S_{21,\text{dB},f2}$ and $S_{21,\text{dB},\text{PIM}}$, respectively. The carrier power fed into the DUT is denoted as $P_{\text{dBm},c}$ (usually, carrier 1 has the same power with carrier 2). Suppose that the PIM power of the DUT $P_{\text{dBm},\text{DUT},\text{PIM}}$ can be described as:

$$P_{\text{dBm},\text{DUT},\text{PIM}} = P_{\text{dBm},0} + kP_{\text{dBm},c}, \quad (1)$$

where $P_{\text{dBm},0}$ and k are constants for a given DUT. Usually, for common passive devices, k ranges from 2 to 3. $P_{\text{dBm},0}$ is the DUT's PIM level when the applied carrier power is 0 dBm. By ignoring the insertion loss from the output port of PIM probes to the input port of SA, the carrier power for carrier 1 $P_{\text{dBm},f1}$ and carrier 2 $P_{\text{dBm},f2}$ entering into the SA should be:

$$P_{\text{dBm},f1} = P_{\text{dBm},c} + S_{21,\text{dB},f1}, \quad (2)$$

$$P_{\text{dBm},f2} = P_{\text{dBm},c} + S_{21,\text{dB},f2}. \quad (3)$$

Since $S_{21,\text{dB},f1}$ is usually different from $S_{21,\text{dB},f2}$, the carrier power going into the SA will be different. The PIM power generated by the DUT and entering into the SA $P_{\text{dBm},\text{PIM}}$ is:

$$P_{\text{dBm},\text{PIM}} = P_{\text{dBm},\text{DUT},\text{PIM}} + S_{21,\text{dB},\text{PIM}}. \quad (4)$$

As mentioned above, when dual tone carriers go into the SA, the intermodulation of the SA, $P_{\text{dBm,SA,PIM}}$, may be excited and it can be described as:

$$P_{\text{dBm,SA,PIM}} = P_{\text{dBm,1}} + k_1 P_{\text{dBm,f1}} + k_2 P_{\text{dBm,f2}}. \quad (5)$$

Similar to Eq. (1), $P_{\text{dBm,1}}$, k_1 , and k_2 are constants for a given SA. In case of the third order PIM with a lower band, $f_{\text{pim}} = 2f_1 - f_2$, $k_1 \approx 2$ and $k_2 \approx 1$.

As described above, there are two PIM products presented in SA. One is the PIM generated by DUT and coupled into SA $P_{\text{dBm,PIM}}$. The other is the PIM generated by SA, $P_{\text{dBm,SA,PIM}}$. Another factor influencing PIM tests is the noise floor of SA, $P_{\text{dBm,SA,Noise}}$. Depending on the specifications and measurement setup of SA and the input carrier power $P_{\text{dBm,f1}}$ and $P_{\text{dBm,f2}}$, $P_{\text{dBm,SA,PIM}}$ can be either higher than or lower than $P_{\text{dBm,SA,Noise}}$. Their maximum value determines the sensitivity of PIM tests. Considering that the nonlinearity of SA is more likely to be a problem in PIM tests, we assume $P_{\text{dBm,SA,PIM}} > P_{\text{dBm,SA,Noise}}$ in the following analysis. Considering the 10 dB rule, the following condition should be satisfied if one wants to obtain the accurate results of DUT's PIM:

$$P_{\text{dBm,SA,PIM}} + 10 < P_{\text{dBm,PIM}}. \quad (6)$$

Namely, the PIM level generated by DUT and coupled into SA should be at least 10 dB higher than the PIM level of SA excited by coupled carriers. By introducing Eqs. (1) – (5) into Eq. (6), we can obtain:

$$P_{\text{dBm,0}} + kP_{\text{dBm,c}} + S_{21,\text{dB,PIM}} > P_{\text{dBm,1}} + (k_1 + k_2)P_{\text{dBm,c}} + k_1 S_{21,\text{dB,f1}} + k_2 S_{21,\text{dB,f2}} + 10. \quad (7)$$

In a standard PIM test, $P_{\text{dBm,c}}$ is usually set as 43 dBm. For a given PIM test system, $P_{\text{dBm,1}}$, k_1 and k_2 are constants. For a given DUT, $P_{\text{dBm,0}}$ and k are constants. $S_{21,\text{dB,PIM}}$, $S_{21,\text{dB,f1}}$ and $S_{21,\text{dB,f2}}$ are constants related with PIM probes. They depend on both the design and the setup (e. g., lift-off distance) of the probe. We introduce $\Delta S_{21,\text{dB,f1}}$ and $\Delta S_{21,\text{dB,f2}}$ as measure of the frequency selectivity of the proposed filtering probe:

$$\begin{cases} \Delta S_{21,\text{dB,f1}} = S_{21,\text{dB,PIM}} - S_{21,\text{dB,f1}} \\ \Delta S_{21,\text{dB,f2}} = S_{21,\text{dB,PIM}} - S_{21,\text{dB,f2}} \end{cases}. \quad (8)$$

So, $\Delta S_{21,\text{dB,f1}}$ and $\Delta S_{21,\text{dB,f2}}$ represent differences of coupling strength between carriers and PIM. By introducing Eq. (8) into Eq. (7), one can obtain:

$$S_{21,\text{dB,PIM}}(1 - k_1 - k_2) > -P_{\text{dBm,0}} + P_{\text{dBm,1}} + (k_1 + k_2 - k)P_{\text{dBm,c}} + 10 - k_1 \Delta S_{21,\text{dB,f1}} - k_2 \Delta S_{21,\text{dB,f2}}. \quad (9)$$

Define $C_0 = P_{\text{dBm,1}} - P_{\text{dBm,0}} + (k_1 + k_2 - k)P_{\text{dBm,c}} + 10$, and Eq.(9) can be written as:

$$S_{21,\text{dB,PIM}} < \frac{k_1 \Delta S_{21,\text{dB,f1}} + k_2 \Delta S_{21,\text{dB,f2}} - C_0}{k_1 + k_2 - 1}. \quad (10)$$

To interpret Eq.(10), we take the third order PIM $2f_1 - f_2$ as an example to give a case study, and it can be supposed that: $P_{\text{dBm,1}} = 45$, $P_{\text{dBm,0}} = -20$, $k_1 = 2$, $k_2 = 1$, $k = 3$, and $P_{\text{dBm,c}} = 43$. Thus, Eq. (10) can be written as:

$$S_{21,\text{dB,PIM}} < \frac{2\Delta S_{21,\text{dB,f1}} + \Delta S_{21,\text{dB,f2}} - 75}{2}. \quad (11)$$

For the non-filtering probe ($\Delta S_{21,\text{dB,f1}} = \Delta S_{21,\text{dB,f2}} = 0$), Eq. (11) becomes:

$$S_{21,\text{dB,PIM}} < -37.5. \quad (12)$$

For the filtering probe, suppose $\Delta S_{21,\text{dB,f1}} = 10$, $\Delta S_{21,\text{dB,f2}} = 15$, and Eq. (11) becomes:

$$S_{21,\text{dB,PIM}} < -20. \quad (13)$$

Eqs. (12) and (13) indicate that the coupling strength of non-filtering/filtering probes should be weaker than $-37.5/-20$ dB, respectively. In other words, a filtering probe can be designed with stronger coupling strength than a non-filtering probe. So, we can conclude that a filtering probe has higher sensitivity than a non-filtering probe.

Eq. (9) can be used as a guide for designing PIM test systems. It relates the system's performance with DUT, SA/receiver, and applied carrier power. The most important point is that it shows how filtering probes' frequency selectivity interacts with systems' sensitivity. More quantitative versions of Eq. (9) can be determined after obtaining the related constants from experimental measurements.

3 Verifications and Discussions

3.1 Design and Simulation

Electromagnetic simulations are conducted to obtain an optimized design of the filtering PIM probe. The resonant frequency is mainly determined by the length of the half-wavelength coaxial transmission line resonator. The small air gap between the inner conductor of the half-wavelength resonator and the inner conductor of the feed connector determines the depth of resonant peaks. Finally, the design of a filtering probe that works around 1 800 MHz is obtained. The total length of the resonator is 68 mm. It should be noted that part of the resonator is filled with Teflon which has a relative dielectric constant ≈ 2 . This dielectric filling will make the resonator a bit shorter than an all air-filled resonator.

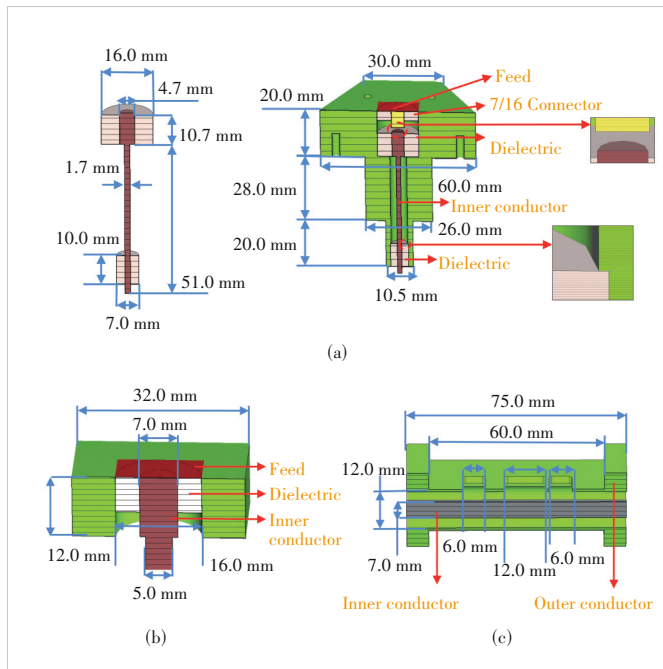
For comparison, we also simulate a commercially available RF connector (model: L29-kfd-9) as a non-filtering PIM probe. A coaxial transmission line with a perforated outer conductor is simulated as DUT. In simulation, the coupling strength of the probe can be adjusted by tuning the lift-off distance. The lift-off distance is swept from 0 to 4 mm with a step of 1 mm. The schematic view and size of the DUT and probes are shown in Fig. 4. The inner conductor of the resonator is fixed by two dielectric rings, which are fixed by the interference fit.

Compared with the non-filtering probe, as shown in Fig. 5, the filtering probe has frequency selectivity as expected. In addition, for both probes, the coupling strength increases as lift-off distance decreases. As analyzed above, this frequency selectivity is helpful to low PIM tests as well as PIM tests at high carrier power. In addition, it can be referred that the lift-off distance is an important factor in the PIM test.

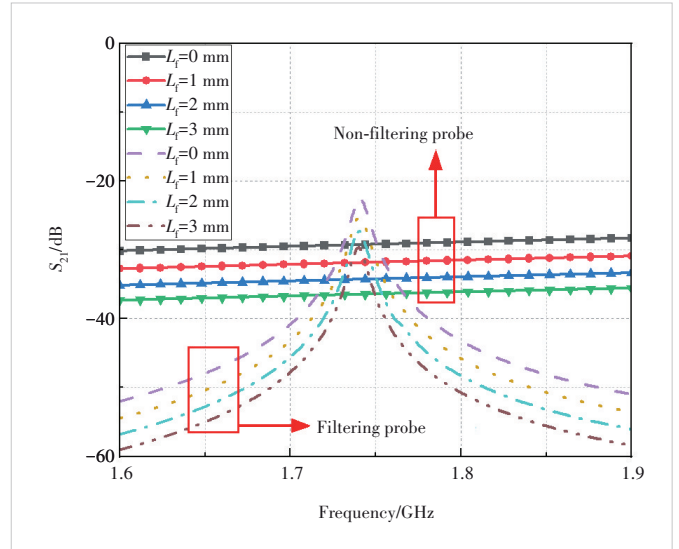
A more detailed comparison is given in Fig. 6. The difference of S_{21} in the filtering probe and non-filtering probe at the PIM frequency of 1.74 GHz is 0.2 dB. Thus, it is considered that the coupling strength of the two probes at the PIM frequency is the same. From Fig. 6, we can find that at carrier 1 (1.81 GHz), $\Delta S_{21, dB, f1} = 22.3$ dB, while at carrier 2 (1.88 GHz), $\Delta S_{21, dB, f2} = 28.9$ dB. Therefore, as for suppressing excitation of the intermodulation of SA, the filtering probe has an advantage over the non-filtering probe.

3.2 Experiments

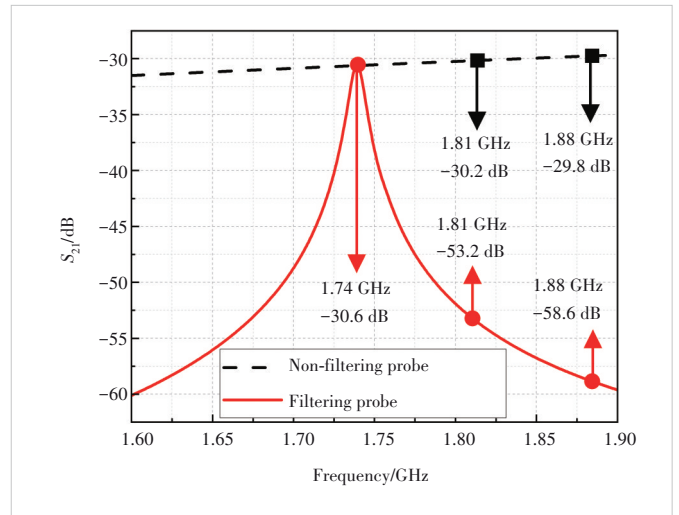
To verify the analysis/simulation mentioned above, a fil-



▲ Figure 4. Simulation model and size of (a) filtering probe, (b) non-filtering probe and (c) DUT (the DIN connector is neglected)

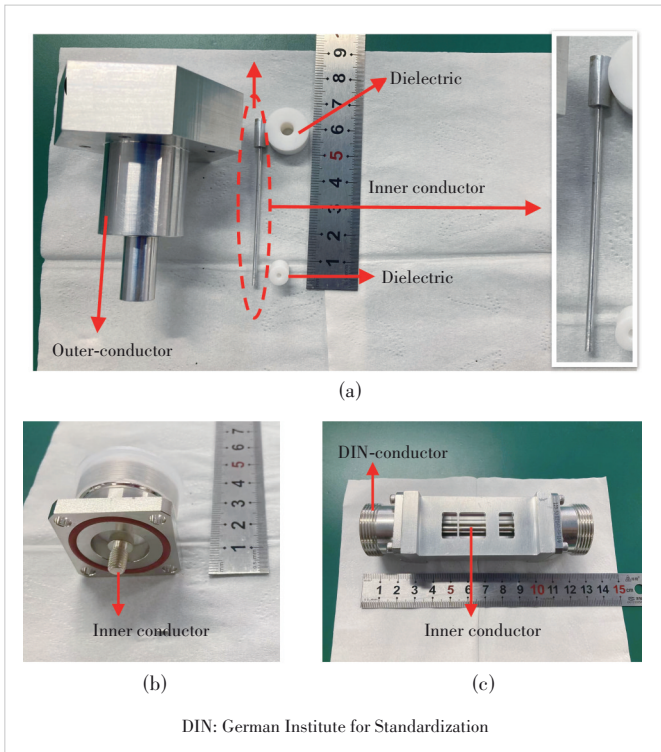


▲ Figure 5. Simulation results on transmission S_{21} between the input port of DUT and the output port of PIM probe (L_r represents lift-off distance)



▲ Figure 6. A detailed comparison of S_{21} in the filtering probe and the non-filtering probe

tering probe and a slotted coaxial line are fabricated by the standard computer numerical control (CNC) process, as shown in Fig. 7. To reduce the PIM level of the probe, it is recommended that non-magnetic metal or metallic coating (such as silver) should be used and metallic contact should be avoided. A commercially available L29-kfd-9 connector is used as a non-filtering PIM probe. A specially designed coaxial transmission line is used as DUT. The outer conductor is perforated to facilitate near-field PIM detection. The inner conductor is electroplated with a nickel of $15 \mu\text{m}$ to introduce strong nonlinearity. To accurately control the probe position, especially the lift-off distance, some mechanic setups are used. As mentioned above, the inner conductor of the filtering probe is fixed inside the probe using two Teflon dielectric rings. We have measured S_{11} of the filtering probe



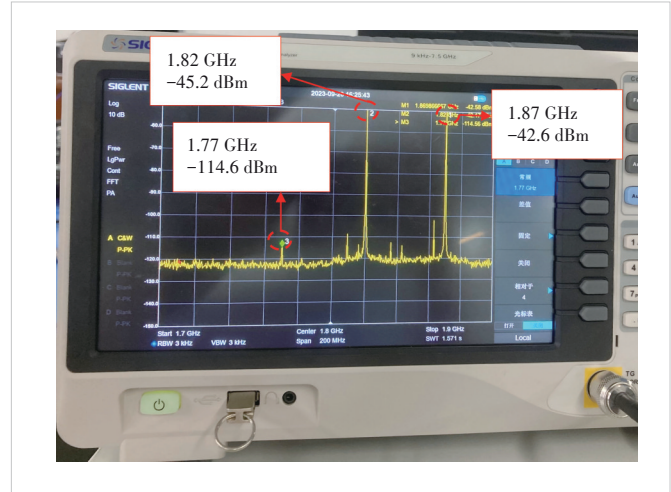
▲ Figure 7. Fabricated (a) filtering probe, (b) non-filtering probe and (c) DUT

without DUT as well as S_{21} when the probe is loaded with DUT. These measurement results show similar behavior with simulations.

Using the slotted coaxial line as DUT, a preliminary near-field PIM test was carried out using a home made PIM setup working at the DCS1800 (a digital cellular system working at 1 800 MHz) band. First of all, we measured the nonlinearity of the SA and obtained results show when the carrier power fed into SA was lower than -43 dBm, the intermodulation generated by the SA itself would not affect the PIM test, as shown in Fig. 8. It can be seen that when carrier power is about -42 dBm, the intermodulation of SA can be below -110 dBm.

Next, two groups of measurements were conducted to demonstrate the advantages of the proposed filtering probe. In both groups, the frequency of carriers 1 and 2 is 1 815 MHz and 1 870 MHz, respectively. The third-order PIM at $f_{PIM} = 1.76$ GHz is measured which equals the center frequency of the filtering probe. The lift-off distance is almost the same, namely, around 0.5 mm, for both kinds of probes. The inner conductor of DUT is brass.

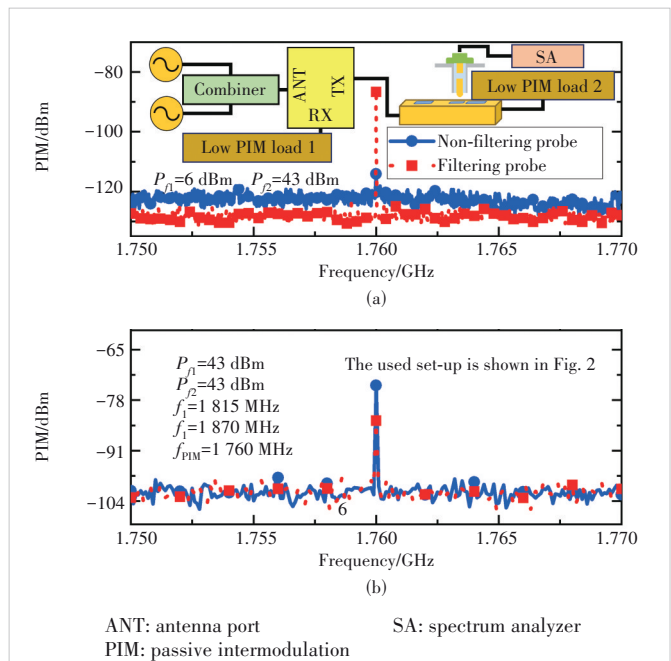
In the first group, we use a test set-up shown in Fig. 9a without the two power amplifiers, duplexer 2 or PIM load 3. Power of carriers input into the DUT is around 6 dBm (enough for exciting the intermodulation of the SA). As shown in Fig. 9a, the observed intermodulation (IM) power is around -115 dBm and -85 dBm for filtering probes and non-filtering probes, respec-



▲ Figure 8. Measurement results of the nonlinearity of the SA

tively. This means that, compared with the non-filtering probe, the power of carriers going into the SA is less for the filtering probe. In other words, compared with the non-filtering probe, the filtering probe brings about more attenuation to carriers, as described in Section 3.1.

In the second group of measurements, the used set-up is the same with the set-up shown in Fig. 2. The conductive foam with strong RF nonlinearity is placed onto the inner conductor of the perforated coaxial transmission line. At the PIM frequency, the observed coupling loss of non-filtering



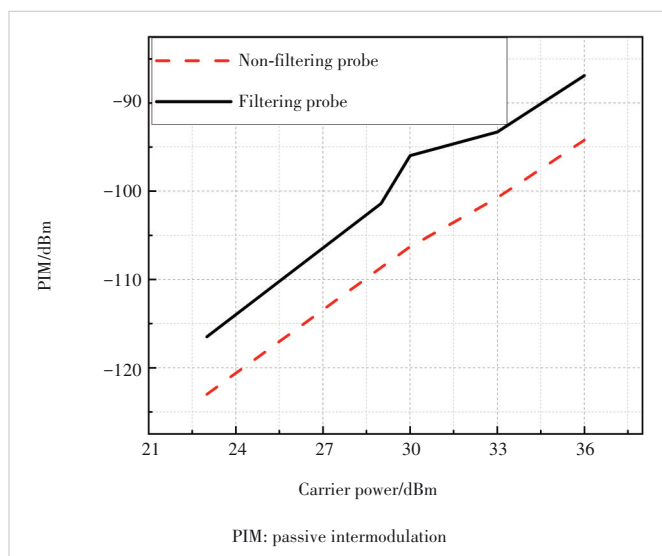
▲ Figure 9. Two groups of measurements: (a) the first group and (b) the second group

probes is higher than that of filtering probes. Thus, the directly measured PIM of the filtering probe is higher than that of the non-filtering probe, as shown in Fig. 9b. Carrier power input into DUT is set to 43 dBm. The PIM level is about -74.4 dBm for the filtering probe and about -84.5 dBm for the non-filtering probe. So, it is demonstrated that the proposed filtering probe has a stronger coupling capability to the DUT's PIM than non-filtering probes. Thus, it can be inferred that the filtering probe shows higher sensitivity or larger dynamic range than non-filtering probes.

Finally, we use the same lift-off distance for both the filtering probe and non-filtering probe and compare their PIM test performance, as shown in Fig. 10. The observed PIM level of the filtering probe is significantly higher than that of the non-filtering probe. Thus, it can be concluded that the filtering probe shows higher sensitivity or larger dynamic range than the non-filtering probe.

4 Conclusions

A filtering PIM probe is proposed for near-field PIM tests. Both simulations and measurements show that the filtering probe has potential advantages compared with conventional non-filtering probes. When the same coupling strength for PIM is obtained, the suppression of carrier power of filtering probes can be about 20 dB higher than that of non-filtering probes. Preliminary results also show that the dynamic range of filtering probes is larger than that of non-filtering probes, which indicates the filtering probe can measure lower PIM products than non-filtering probes. Another potential benefit of using a filtering probe is that it can relax the requirement for the duplexer and receiver of PIM test systems, which will help with system integration and cost reduction.



▲ Figure 10. Measured dependence of PIM on carrier power for both the filtering and non-filtering probes

References

- [1] BAYRAK M, BENSON F A. Intermodulation products from nonlinearities in transmission lines and connectors at microwave frequencies [J]. *Proceedings of the institution of electrical engineers*, 1975, 122(4): 361. DOI: 10.1049/piee.1975.0101
- [2] GOLIKOV V, HIENONEN S, VAINIKAINEN P. Passive intermodulation distortion measurements in mobile communication antennas [C]// *The 54th Vehicular Technology Conference*. IEEE, 2001: 2623 - 2625. doi: 10.1109/VTC.2001.957226
- [3] HOEBER C, POLLARD D, NICHOLAS R. Passive intermodulation product generation in high power communications satellites [C]// *The 11th Communications Satellite Systems Conference*. AIAA, 1986: 657. DOI: 10.2514/6.1986-657
- [4] SHITVOV A P, KOZLOV D S, SCHUCHINSKY A G. Nonlinear characterization for microstrip circuits with low passive intermodulation [J]. *IEEE transactions on microwave theory and techniques*, 2018, 66(2): 865 - 874. DOI: 10.1109/tmtt.2017.2758726
- [5] SHITVOV A, SCHUCHINSKY A G, STEER M B, et al. Characterisation of nonlinear distortion and intermodulation in passive devices and antennas [C]// *The 8th European Conference on Antennas and Propagation (EuCAP 2014)*. IEEE, 2014: 1454 - 1458. DOI: 10.1109/eu-cap.2014.6902055
- [6] KIMINO T, KUGA N. Basic consideration on non-contact localization for a PIM source in array antenna [C]// *International Symposium on Antennas and Propagation (ISAP)*. IEEE, 2021: 395 - 396. DOI: 10.23919/isap47053.2021.9391124
- [7] GOPALAN R, LENG L J, KOMINEK S, et al. Generalized virtual PIM measurement for enhanced accuracy: US11374661 [P]. 2022-06-28
- [8] SHITVOV A P, ZELENCHUK D E, SCHUCHINSKY A G, et al. Passive intermodulation generation on printed lines: Near-field probing and observations [J]. *IEEE transactions on microwave theory and techniques*, 2008, 56(12): 3121 - 3128. DOI: 10.1109/tmtt.2008.2007136
- [9] CAI Z H, LIU L, DE PAULIS F, et al. Passive intermodulation measurement: challenges and solutions [J]. *Engineering*, 2022, 14: 181 - 191. DOI: 10.1016/j.eng.2022.02.012
- [10] TARIQ R U, YE M, ZHANG K Y, et al. Wide-band high dynamic range variable passive intermodulation generator using fabric-over-foam gasket [J]. *International journal of electronics and communications*, 2020, 126: 153400. DOI: 10.1016/j.aeue.2020.153400
- [11] SHITVOV A P, ZELENCHUK D E, OLSSON T, et al. Transmission/reflection measurement and near-field mapping techniques for passive intermodulation characterisation of printed lines [C]// *The 6th International Workshop on Multipactor, Corona and Passive Intermodulation in Space RF Hardware, MULCOPIM*, 2008: 1 - 6
- [12] CHEN Z Y, ZHANG Y, DONG S Q, et al. Wideband architecture for passive intermodulation localization [C]// *MTT-S International Wireless Symposium (IWS)*. IEEE, 2018: 1 - 3. DOI: 10.1109/ieeee-iws.2018.8400921
- [13] YANG S, WU W, XU S, et al. A passive intermodulation source identification measurement system using a vibration modulation method [J]. *IEEE transactions on electromagnetic compatibility*, 2017, 59(6): 1677 - 1684. DOI: 10.1109/TEMC.2017.2705114
- [14] YONG S H, YANG S, ZHANG L, et al. Passive intermodulation source localization based on emission source microscopy [J]. *IEEE transactions on electromagnetic compatibility*, 2020, 62(1): 266 - 271. DOI: 10.1109/TEMC.2019.2938634
- [15] HIENONEN S, GOLIKOV V, MOTTONEN V S, et al. Near-field amplitude measurement of passive intermodulation in antennas [C]// *The 31st European Microwave Conference*. IEEE, 2001: 1 - 4. DOI: 10.1109/EUMA.2001.339019
- [16] CHEN X, AN L, YU M, et al. Waveguide cell with water filling for passive intermodulation localization on planar circuits [J]. *IEEE microwave and wireless components letters*, 2021, 31(11): 1247 - 1250. DOI: 10.1109/LMWC.2021.3090081

Biographies

BAI Yongjiang received his BS degree in computer science and technology science from Shangrao Normal University, China in 2021. He is currently with Xi'an University of Architecture and Technology, China. His research interests include passive intermodulation and microwave rotational speed measurement. He has published 7 papers in various journals and conferences.

YANG Jiye received his BS degree in electronic information from Xi'an University of Architecture and Technology, China in 2023. He is currently with Xi'an University of Architecture and Technology. His research interests include passive intermodulation detection and microwave measurement.

ZHU Shaohao obtained his PhD degree in underwater acoustic engineering from Northwestern Polytechnical University, China in 2021. He is currently serving as an RF algorithm engineer at ZTE Corporation. His research interests encompass a wide range of cutting-edge topics, including passive intermodulation (PIM) mechanisms, PIM cancellation techniques, source localization, array beamforming, and satellite navigation and positioning technologies. With a robust background in both theoretical and practical aspects of

RF engineering, he is dedicated to advancing the field through innovative research and development.

YANG Ye received his master's degree in electromagnetic field and microwave from Xidian University, China in 2013. He is currently working at ZTE Corporation as an antenna feeder development engineer. His research mainly focuses on base station antenna design and development, including base station antenna PIM elimination and suppression, antenna pattern optimization and forming, active and passive antenna integration, and green antennas.

YE Ming (yeming@xauat.edu.cn) received his BS degree in information and computation science from Chongqing University of Posts and Telecommunications, China in 2008, and his MS and PhD degrees in electronic science and technology from Xi'an Jiaotong University, China in 2010 and 2014, respectively. He is currently with Xi'an University of Architecture and Technology, China. His research interests include passive intermodulation, secondary electron emission, microwave breakdown, microwave measurement and sensors. He has published around 100 papers in various journals and conferences.